

Phase-matched high-order-harmonic generation in a gas-filled hollow fiber

Yusuke Tamaki,* Yutaka Nagata, Minoru Obara,* and Katsumi Midorikawa†

Laser Technology Laboratory, The Institute of Physical and Chemical Research (RIKEN), 2-1 Hirosawa, Wako-shi, Saitama 351-0198, Japan

(Received 24 July 1998)

Phase-matched high-order-harmonic generation of Ti:sapphire laser pulses of $\approx 10^{14}$ W/cm² has been demonstrated using a gas-filled hollow fiber. The high-order-harmonic spectrum emitted from the fiber showed an intensity distribution significantly different from that in free space, indicating more than a hundred times enhancement around the 25th harmonic. A simple phase-matching calculation considering positive dispersion due to plasma and negative dispersion due to neutrals indicates that macroscopic phase matching achieved in the fiber is responsible for the strong enhancement. [S1050-2947(99)08305-5]

PACS number(s): 42.65.Ky, 32.80.Rm

High-order-harmonic generation (HHG) [1–4] has been extensively studied since it has a promising potential for a coherent extreme ultraviolet (XUV) and soft-x-ray source. XUV light produced by the HHG technique has excellent temporal resolution, which allows dynamic studies of such as XUV spectroscopy and photoelectron spectroscopy. So far, investigations of HHG have been focused on the increase in cutoff frequency and the enhancement of XUV intensity in the plateau region in order to obtain a widely tunable coherent XUV emission. Recently, Spielmann *et al.* [4] demonstrated continuum XUV emission up to 0.5 keV using three-optical cycle pulses, reaching the “water window” wavelength region. Although the system developed is very compact and table-top size, the number of photons generated is 10^3 per pulse, which is not high enough for various applications. Therefore, the next important step is to determine a method to increase the harmonic intensity to a level high enough for a variety of applications.

In order to improve HHG efficiency, the reduction of phase mismatch between the pump and harmonic waves is crucial. Unfortunately, few studies have so far attempted to address the phase-matching issue in a plasma and neutral gas mixture, since the investigation of the phase-matching condition is difficult due to complicated phenomena such as self-focusing and plasma defocusing [5] in the interaction region with the tight focusing geometry employed. Although Gaarde *et al.* [6] reported the effects of macroscopic phase matching through propagation numerically, they neglected the dispersion effects induced by ionization.

Recently, several techniques to control the propagation conditions of intense ultrafast laser pulses were investigated. These include the formation of plasma columns in gases based on bulk plasma motion [7], relativistic electron oscillation [8], balance between self-focusing and diffraction of a laser beam [9,10], or reflection from a plasma lining wall [11]. Using a glass-coated hollow-core fiber, Nisoli *et al.*

[12] demonstrated the long channeling of intense, femtosecond laser pulses at an intensity of 10^{13} W/cm².

Using the hollow waveguide, we demonstrated the third harmonic generation of an intense, femtosecond Ti:sapphire laser pulse [13], where the improvement of phase matching and beam quality was demonstrated clearly. The observations motivated us to further investigate the higher-order-harmonic generation in the XUV regime using a hollow fiber [14,15].

In this paper, we report the demonstration of phase-matched HHG of Ti:sapphire laser pulses in a fused-silica clad hollow-core fiber. The high-order-harmonic spectrum emitted from the fiber filled with argon gas shows an intensity distribution significantly different from that in free space. By comparing the two harmonic distributions, we observed more than a hundred times enhancement around the 25th harmonic with the hollow fiber. A simple phase-matching calculation considering positive dispersion due to plasma and negative dispersion due to neutrals indicates that the strong enhancement is attributed to a macroscopic phase matching achieved in the hollow fiber.

The laser pulses used in this study were generated by a chirped-pulse-amplification based Ti:sapphire laser producing 80 fs temporal length with 4 mJ energy at 10-Hz repetition rate. The measured confocal parameter was 0.4 cm. The amplified pulses were focused with an $f=50$ cm achromatic lens to 90 μm in diameter behind a pinhole of a static gas cell in a vacuum chamber (Fig. 1). Laser pulses were focused in front of the fiber. The fiber and the two pinholes were positioned by observing the output fundamental beam pattern with an infrared fluorescent card that was set in front of the spectrometer slit 1 m apart from the fiber end. The maximum coupling efficiency to the fiber for a single mode was 50%, which was lower than the theoretical efficiency of 90% calculated with the experimental value of $w_0/a=0.75$, where w_0 is the waist of the diameter of the input beam and a is the bore diameter of the hollow fiber. The fiber length was determined from the conditions that the propagation loss could be neglected. The hollow fiber employed had a bore diameter of 126 μm and the clad part was made of fused silica with 1.8 mm outer diameter. The fiber was originally fabricated for use as a connector of single-mode fibers. The fiber did not suffer from any damage during the experiment that was

*Present address: Department of Electronics and Electrical Engineering, Keio University, 3-14-1 Hiyoshi, Kohoku, Yokohama 223-8522, Japan.

†Electronic address: kmidori@postman.riken.go.jp

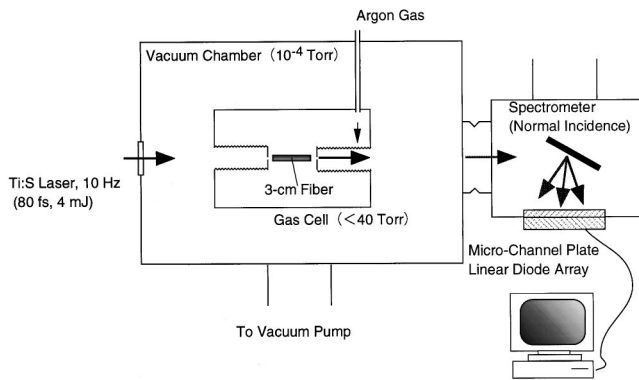


FIG. 1. Schematic of the top view of a differential-pumped gas cell. The focusing lens ($f=50$ cm) is located at the outside of the vacuum window. Emitted harmonics pass through the $100\ \mu\text{m}$ slit and are dispersed with a normal incidence, platinum-coated grating. The dispersed XUV light is converted into visible lights with a microchannel plate and a photocathode. The visible light is detected by a cooled, fiber-coupled 1D CCD array.

performed for several hours, when the incident beam and the hollow fiber were properly aligned on the optical axis. The gas cell had two $200\text{-}\mu\text{m}$ -diameter pinholes on each end surface of the bellow arms. When the gas cell was pressurized with Ar, the conductance of the pinholes confined the gas to the cell. Thus, the pinholes isolated vacuum and gas-filled regions. The outside of the gas-filled region was maintained at pressures below 10^{-4} Torr when the cell was pressurized at 20 Torr. The hollow fiber was placed on the V groove mounter in the gas cell. The positioner controlled from the outside of the cell allowed easy change of the distance between two pinholes, which made it possible to find the optimum distance for free space experiments.

Harmonic signals from the fiber were observed with a flat-field normal-incident XUV spectrograph with a platinum-coated concave grating blazed at $60\ \text{nm}$ (1200 lines/mm). This spectrograph equipped with a microchannel plate detector can cover the spectral ranges from 30 to $80\ \text{nm}$ and from 80 to $120\ \text{nm}$ by changing the position of the microchannel detector. In this experiment, we used the range from 30 to $80\ \text{nm}$ and all data were acquired using an integration time of ten seconds at $10\ \text{Hz}$. Line spectra appearing at both sides of the 11th and the 13th harmonic in Fig. 2(a) are the second-order diffraction lights of the 21st to the 27th harmonic. Experimental conditions such as applied voltages were the same. Therefore, the spectra of both experiments can be compared directly. Noisier background in Fig. 2(a) came from the plasma fluorescence of laser and fiber-wall interaction.

The spectral distributions from the 11th to the 27th harmonic with and without the hollow fiber showed remarkable differences (Fig. 2). The spectral intensities in free space decreased gradually with increasing the harmonic order, while those with the fiber decreased steeply from the 11th to the 17th harmonic and markedly increased from the 21st to 27th harmonic. When detection efficiency is considered, the spectrum in Fig. 2(b) would show a plateau in the distribution, because the intensity of the fundamental laser was sufficiently high to produce a plateau in this wavelength region. This is also supported by the fact that the relative diffraction efficiency of the employed grating ($60\ \text{nm}$ blazed) almost

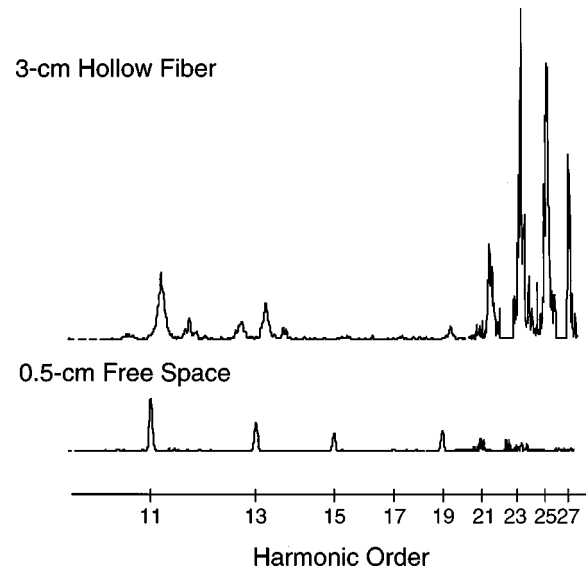


FIG. 2. Observed harmonic spectral distribution emerging (a) from a $3\ \text{cm}$ hollow fiber and (b) in $0.5\ \text{cm}$ free space. Ar gas pressure is $5\ \text{Torr}$. Experimental conditions such as applied voltage to microchannel plate and integration time were all same for both experiments. The horizontal axes were to be scaled.

linearly decreases from one to zero with decreasing wavelength from 60 to $30\ \text{nm}$. Figure 2(a) shows a significant enhancement around the 25th harmonic with the fiber even before the intensity correction by considering the detection efficiency of the equipment. Each harmonic spectrum obtained with the fiber was broader and blueshifted compared to that in free space, clearly indicating the propagation effects in the fiber.

As concerning to the absorption effect by the argon gas, we found that no significant absorption was taken place during the interaction. The difference in transmissions between 11th and 25th harmonics seems too big (in the case of 5-Torr , 3-cm thick Ar, the difference is calculated to be 5 orders of magnitudes [16]). However, we still observed both harmonics simultaneously with and without the hollow fiber. The conclusion was that the absorption effects conducted quite differently in strong laser field. That is why we neglect the absorption effect in the following discussions.

The absolute enhancement factor for each harmonic with the fiber was obtained by dividing the harmonic intensities in Fig. 2(a) by those in Fig. 2(b). Figure 3 shows the enhancement factors of the individual harmonics. From the 21st harmonic, the enhancement factor rapidly increased and attained its peak value at the 25th harmonic. The fluctuation between the 15th and 19th harmonic was due to low signal-to-noise ratios because of the low signal intensity with the fiber in this region. It should be noted that despite of the lack of enhancement from the 15th to 19th harmonic, more than 100 times enhancement was obtained at the 25th harmonics with a hollow fiber.

In our experimental geometry, the volume effect can be neglected. Since the harmonics are pumped only on axis, off-axially pumped light can never couple to the fundamental due to a radial intensity distribution which leads to a rapid change of harmonic phase and a strong radial variation of a plasma density; in other words, gain guiding exerts a domi-

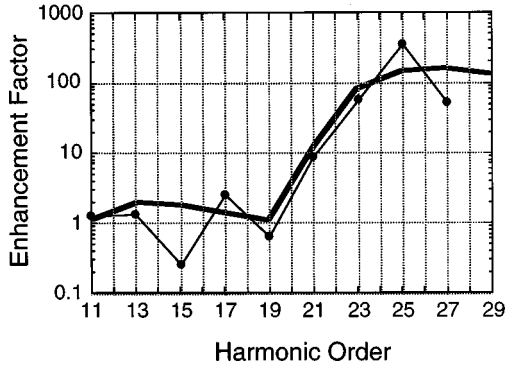


FIG. 3. Experimentally obtained (thin line) and calculated (bold line) enhancement factors as a function of harmonic order.

nant effect on volume in the hollow fiber. Although the pumping laser energy exists over the cross section in the core part, the coupling between pumping and generating fields is limited near the fiber center. Furthermore, we observed same tendency in high-harmonic spectral distribution in an experiment of HHG by a self-guided beam without the hollow fiber [17]. These are the reasons that we neglect the waveguide-induced dispersions in the following calculation. In this interaction region, parameters such as laser intensity and interaction plasma density are considered to be constant. The phase front of the driving laser also remains in the flat. Thus, the calculation of phase matching becomes one dimensional in the fiber.

In order to explain the enhancement around the 25th harmonics, we considered that the macroscopic phase matching played an important role in the hollow fiber. The amount of phase-matching factors of each harmonic can be estimated from the nonperturbation theory [14], which is a powerful method for understanding macroscopic interaction mechanisms. The calculation of the phase-matching factor Δk was carried out based on our previous paper [13] which was used to explain pump intensity dependence of the third harmonic generation. In the calculation, we assumed a model in which the harmonics were pumped at the leading edge of the driving pulses. Appropriateness of this model is indicated by results reported by Zhou *et al.* [3] that the harmonic spectra are shifted in the same direction as the pump pulse chirp direction.

The total amount of phase mismatch of the q th harmonic wave is given by $\Delta k_q = 2\pi(n_q/\lambda_q - qn_f/\lambda_f)$, where n_q and n_f are the refractive indices and λ_q and λ_f are the wavelengths of q th and fundamental waves, respectively. The refractive index for neutral argon $n_{q,\text{neu}}$ consists of linear and nonlinear parts as described below, and those for free electron gases $n_{q,fe}$ are calculated from the plasma frequency. Thus, the total refractive index is expressed by $n_q = n_{q,\text{neu}} + n_{q,fe}$. For the dispersion caused by free electrons, the refractive index of a plasma is given by $n_{q,fe} = \sqrt{1 - (\omega_q^2/\omega_p^2)}$, where ω_q and ω_p are the angular frequencies of the q th harmonic and the plasma waves, respectively.

The refractive index for neutral argon $n_{q,\text{neu}}$ is strongly intensity dependent, and the dependence stems from the nonlinear refractive index n_2 of neutrals (that of ions is extremely low). The refractive index of neutrals, therefore, is expressed as a summation of linear and nonlinear refractive

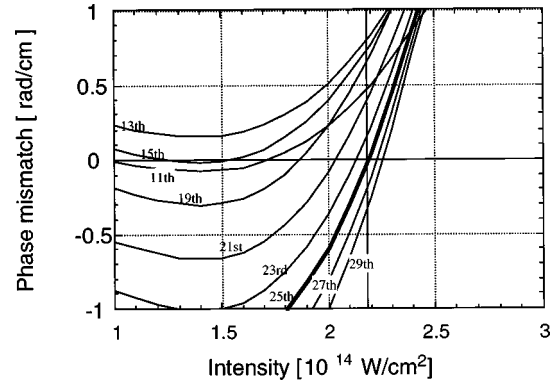


FIG. 4. Total amount of phase mismatch as a function of fundamental laser intensity for various harmonics. Bold line indicates the amount of phase mismatch of the 25th harmonics.

indices $n_{q,\text{neu}} = (n_{q,0} + n_{q,2}I_q)N_{\text{neu}}$, where $n_{q,0}$ represents linear refractive index given in Ref. [1] for noble gases and $n_{q,2}$ is the nonlinear refractive index of $5 \times 10^{-19} \text{ cm}^2/\text{W}$ for infrared light and is neglected for XUV light. Thus, the refractive index of neutral argon is proportional to the density of surviving neutrals N_{neu} during the interaction.

The calculation was made with the above set of equations. As we described, we assumed that the harmonics were pumped 10 fs before the pumping pulse's peak [13], where the interaction intensity was 90% of the pump intensity and the corresponding electron density was 5%. Then, all the parameters were determined with the pump intensity, because the electron density was calculated as a function of the pump intensity with an ADK model [18]. Thus, we could calculate the total phase mismatch with only one parameter of the pump intensity.

The calculated phase mismatch for HHG is shown in Fig. 4 as a function of pump laser intensity. The pump intensity which was used for evaluating the harmonic distribution was determined such that the phase mismatching of the 25th harmonic became zero, because it resulted in the maximum enhancement in the experiment. The value of $2.2 \times 10^{14} \text{ W/cm}^2$ was reasonable from our experimental condition with a consideration of coupling loss of laser pulses.

Differences in the amount of phase mismatch between harmonics are small and well within 1 cm^{-1} . To calculate the harmonic intensity distribution out of the fiber, we assumed that the harmonic intensity distribution near the input end of the fiber is constant. This is valid because we obtained a plateaulike distribution in the 5-mm long free space, considering the diffraction efficiency of the grating. Once the harmonic is generated, the output intensity of the q th harmonic at the exit end of the fiber is proportional to $\text{sinc}^2(\Delta k_q L/2)$. This is the so-called phase-matching factor. In order to obtain the intensity distribution at the detector, we should also include the effect of beam divergence, which is proportional to $1/\lambda_q^2$.

The calculated enhancement factor as a function of harmonic order is shown by a bold line in Fig. 3. The enhancement factors are correspondent to the relative spectral intensities of the harmonics when we assume that the intensity distribution of the harmonics in free space is almost constant. The calculated distribution of the enhancement factor is in

good agreement with the experimentally obtained one. As shown in Fig. 3, the strong enhancement of the harmonic intensity around the 25th harmonics is well explained by calculating the macroscopic phase matching in a hollow fiber.

The reason why we have successfully obtained phase-matched harmonics around the 25th harmonics might also be supported by taking account of the intrinsic phase variation of the harmonic [6] when the harmonic is generated. The effect of phase distortion becomes relatively small in the cutoff region, which increases coherence length. Because the macroscopic phase-matching condition is satisfied in the hollow fiber as described above, a smaller variation of the intrinsic phase of the harmonics near the cutoff region is expected to lead phase-matched propagation. Consequently, only the harmonic waves near the cutoff region might be preferentially enhanced.

In conclusion, phase-matched high-order-harmonic generation was demonstrated by using a gas-filled hollow fiber. The guided region was filled with low-pressure argon gas. More than 100 times enhancement around the 25th harmonic was obtained. We determined that phase matching could be achieved by compensating the positive phase mismatch due to free electrons by the negative phase mismatch due to the nonlinear refractive index change of the fundamental. These results open the possibility of a highly efficient coherent XUV source at a high repetition rate. Thus, the high-harmonic generation technique will become a unique and powerful tool in the XUV region.

We would like to acknowledge the technical assistance rendered by O. Maya. We also acknowledge Dr. J. Itatani for thoughtful comments. One of the authors was supported by a grant from the Junior Research Associate Program of RIKEN.

-
- [1] A. L'Huillier, X. F. Li, and L. A. Lompré, *J. Opt. Soc. Am. B* **7**, 527 (1990).
- [2] J. J. Macklin, J. D. Kmetec, and C. L. Gordon III, *Phys. Rev. Lett.* **70**, 766 (1993).
- [3] J. Zhou, J. Peatross, M. M. Murnane, H. C. Kapteyn, and I. P. Christov, *Phys. Rev. Lett.* **76**, 752 (1996).
- [4] Ch. Spielmann, N. H. Burnett, S. Sartania, R. Koppitsch, M. Schnürer, C. Kan, M. Lenzner, P. Wobrauschek, and F. Krausz, *Science* **278**, 661 (1997).
- [5] P. Monot, T. Auguste, L. A. Lompré, G. Mainfray, and C. Manus, *J. Opt. Soc. Am. B* **9**, 1579 (1992).
- [6] M. B. Gaarde, Ph. Antoine, A. L'Huillier, K. J. Schafer, and K. C. Kulander, *Phys. Rev. A* **57**, 4553 (1998).
- [7] C. G. Durfee III, J. Lynch, and H. M. Milchberg, *Opt. Lett.* **19**, 1937 (1994).
- [8] A. Borisov, A. Borovskiy, V. Korobkin, A. Prokhorov, O. Shiryayev, X. Shi, T. Luk, A. McPherson, J. Solem, K. Boyer, and C. Rhodes, *Phys. Rev. Lett.* **68**, 2309 (1992).
- [9] A. Braun, G. Korn, X. Liu, D. Du, J. Squier, and G. Mourou, *Opt. Lett.* **20**, 73 (1995).
- [10] E. T. J. Nibbering, P. F. Curley, G. Grillon, B. S. Prade, M. A. Franco, F. Salin, and A. Mysyrowicz, *Opt. Lett.* **21**, 62 (1996).
- [11] S. Jackel, R. Burris, J. Grun, A. Ting, C. Manka, K. Evans, and J. Kosakowski, *Opt. Lett.* **20**, 1086 (1995).
- [12] M. Nisoli, S. De Silvestri, O. Svelto, R. Szipöcs, K. Ferencz, Ch. Spielmann, S. Sartania, and F. Krausz, *Opt. Lett.* **22**, 522 (1997).
- [13] Y. Tamaki, K. Midorikawa, and M. Obara, *Appl. Phys. B: Lasers Opt.* **B67**, 59 (1998).
- [14] Y. Tamaki, O. Maya, K. Midorikawa, M. Obara, in *International Quantum Electronics Conference 1998*, Vol. 7; JTUA3 of Technical Digest Series (OSA, Washington, DC, 1998).
- [15] C. G. Durfee III, A. Rundquist, S. Backus, Z. Chang, C. Herne, F. Weihe, M. Murnane, and H. Kapteyn, in *International Quantum Electronics Conference 1998, Postdeadline Papers*, QPD5 (OSA, Washington, DC, 1998); A. Rundquist, C. G. Durfee III, Z. Chang, C. Herne, S. Backus, M. M. Murnane, and H. C. Kapteyn, *Science* **280**, 1412 (1998).
- [16] We obtained XUV properties of argon gas from the web site at URL <http://cindy.lbl.gov/by> The Center for X-Ray Optics (CXRO) at the Lawrence Berkeley National Laboratory (LBNL).
- [17] Y. Tamaki, J. Itatani, Y. Nagata, M. Obara, and K. Midorikawa, *Phys. Rev. Lett.* **82**, 1422 (1999).
- [18] M. V. Ammosov, N. B. Delone, and V. P. Krainov, *Zh. Eksp. Teor. Fiz.* **91**, 2008 (1986); [*Sov. Phys. JETP* **64**, 1191 (1986)].